Supporting Information

Small Molecule Intervention at the Dimerization Interface of Survivin by Novel Rigidized Scaffolds

Tamer M. Ibrahim[1,2*], Christoph Ernst[1], Andreas Lange[1], Susanne Hennig[1] and Frank M. Boeckler[1]

[1]Laboratory for Molecular Design and Pharmaceutical Biophysics, Department of Pharmaceutical and Medicinal Chemistry, Institute of Pharmacy, Eberhard Karls University Tuebingen, Auf der Morgenstelle 8, 72076 Tuebingen, Germany

[2]Pharmaceutical Chemistry Department, Faculty of Pharmacy, Kafrelsheikh University, Kafr El-Sheikh 33516, Egypt

Correspondence: Tamer M. Ibrahim

Pharmaceutical Chemistry Department, Faculty of Pharmacy, Kafrelsheikh University, Kafr El-Sheikh 33516, Egypt

Email tamer.ibrahim2@gmail.com

Table of Contents

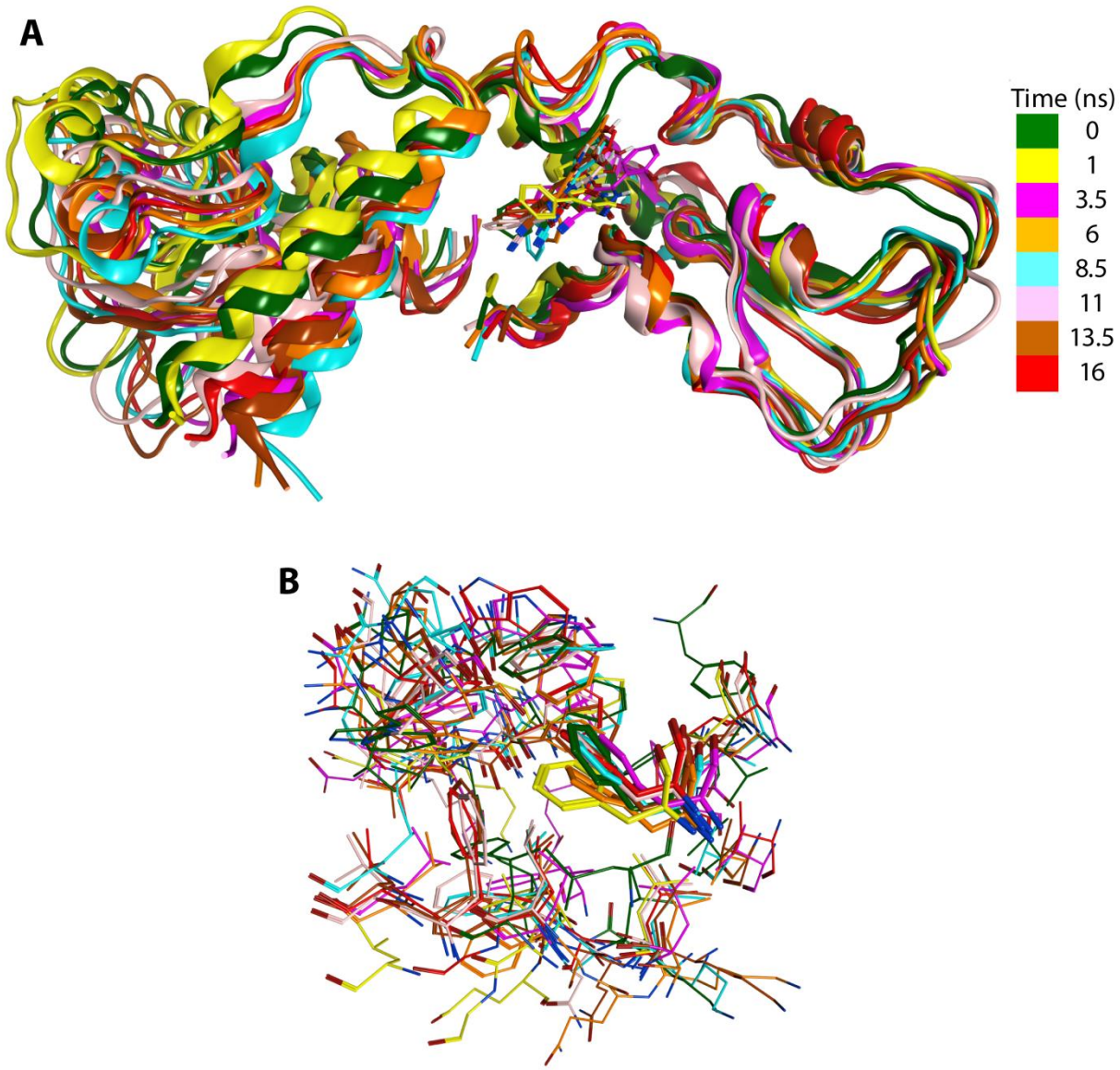

Figure S1. (A) Overview of different MD structures of survivin-Abbott 8 complex at different simulation time (Abbott8 is in sticks representations). (B) Dynamics of the binding site residues (Phe 101 is in sticks representation). The color codes of A and B are similar.

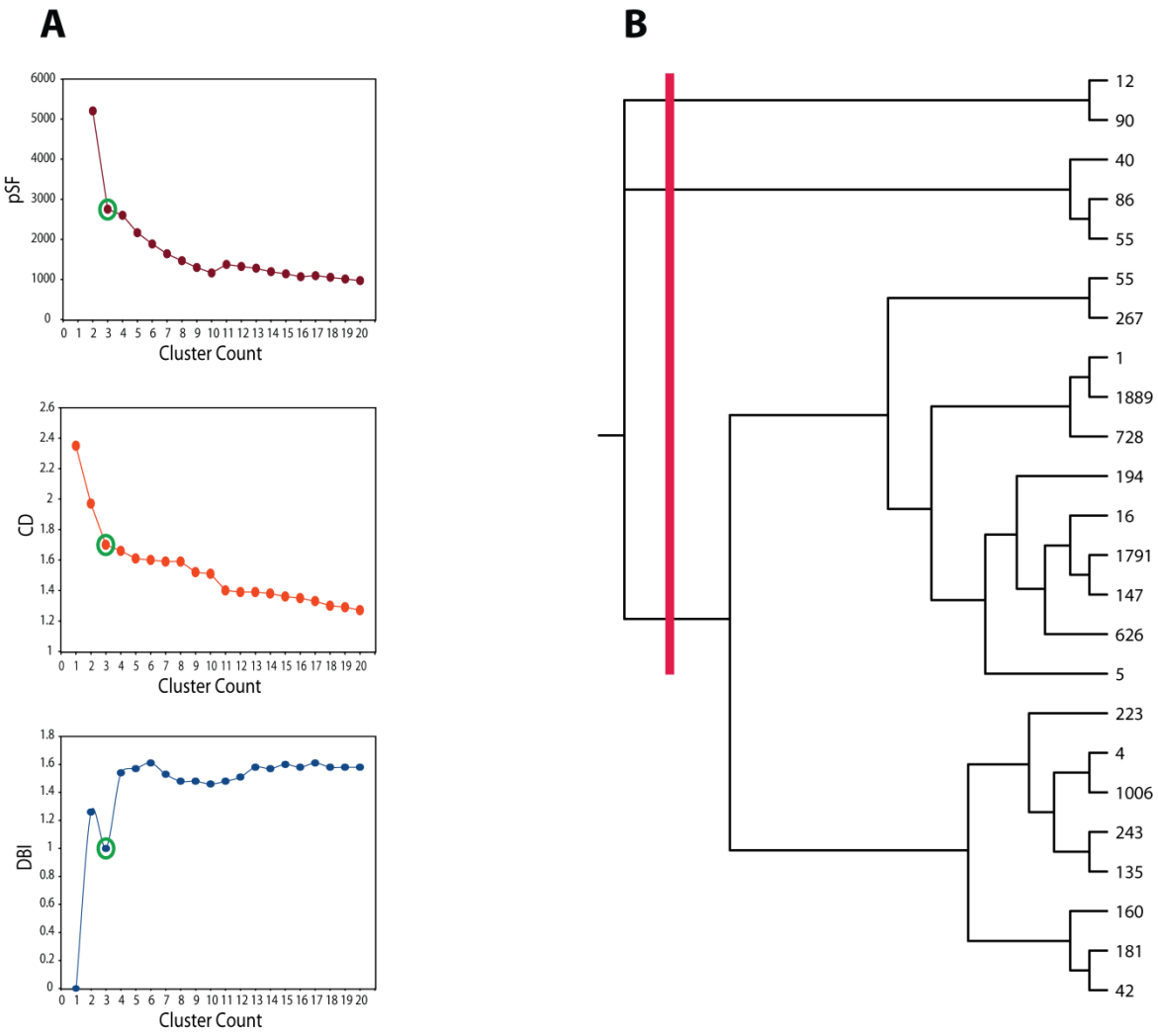

Figure S2. (A) Overview of the metrics used to assess the cluster analysis. The metrics are: pseudo-F Statistic (pSF), Critical Distance (CD) and Davies-Bouldin Index (DBI).[1] The green circle indicates a consensus cluster count of 3. (B) The phenogram of the MD frames (10th frame interval). The red line indicates cluster level of 3.

Cluster analysis based on the "Average-Linkage Algorithm"suggested that the MD frames can be generally presented by three main clusters. Critical distance metric shows a clear transition between clusters 3 to 4. Such transition suggests that there is an obvious separation between clusters for a cluster count of 3 and it is easier to merge higher cluster counts (e.g. 4, 5...etc) to form at the end three clusters. DBI is at its minima with the cluster count of 1 and 3. Since the DBI metric is a direct assessment for the scatter, therefore, it automatically tends to show smaller values when the cluster count decreases. Hence, ignoring the minimum value of DBI at cluster count of 1 helps to minimize this bias and therefore cluster count of 3 is considered. The pseudo F statistics (pSF) is at maxima when the

cluster count is at 2 and 3, however, the peak or the elbow-like transition can be clearly seen at cluster count of 3. Taking a consensus solution between these metrics would suggest that the MD frames can be clustered by three main clusters (cluster count of 3).

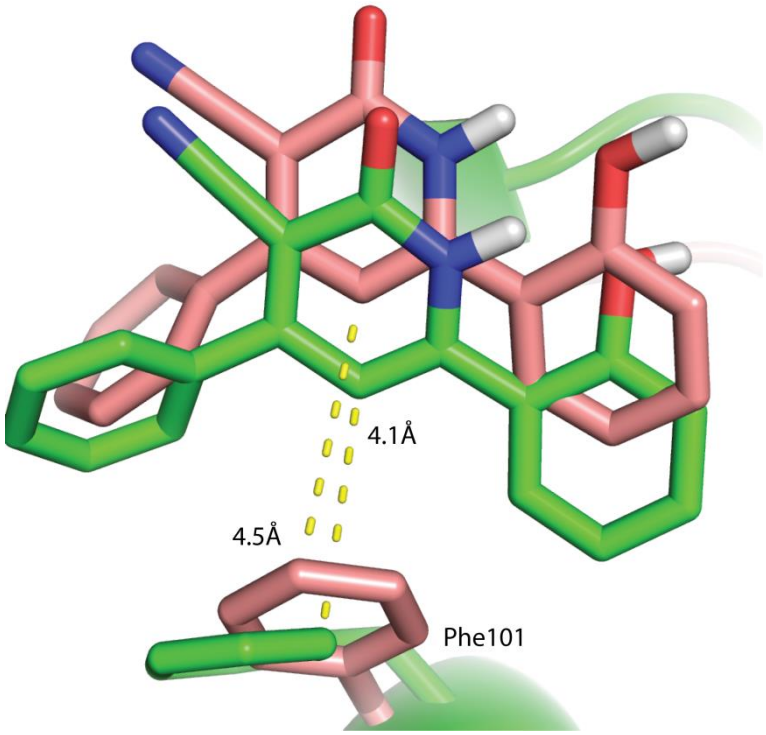

Figure S3. Superposition of the starting structure (green) and the main MD representative structure (pale pink) of survivin-Abbott8 complex. A better distance of position C5 of the pyridone ring towards the Phe101 side chain was found for the main MD representative structure (4.5 Å) versus 4.1 Å for the starting structure. The distance is measured towards the nearest carbon atom of Phe101. Non-polar hydrogens are omitted for clarity.

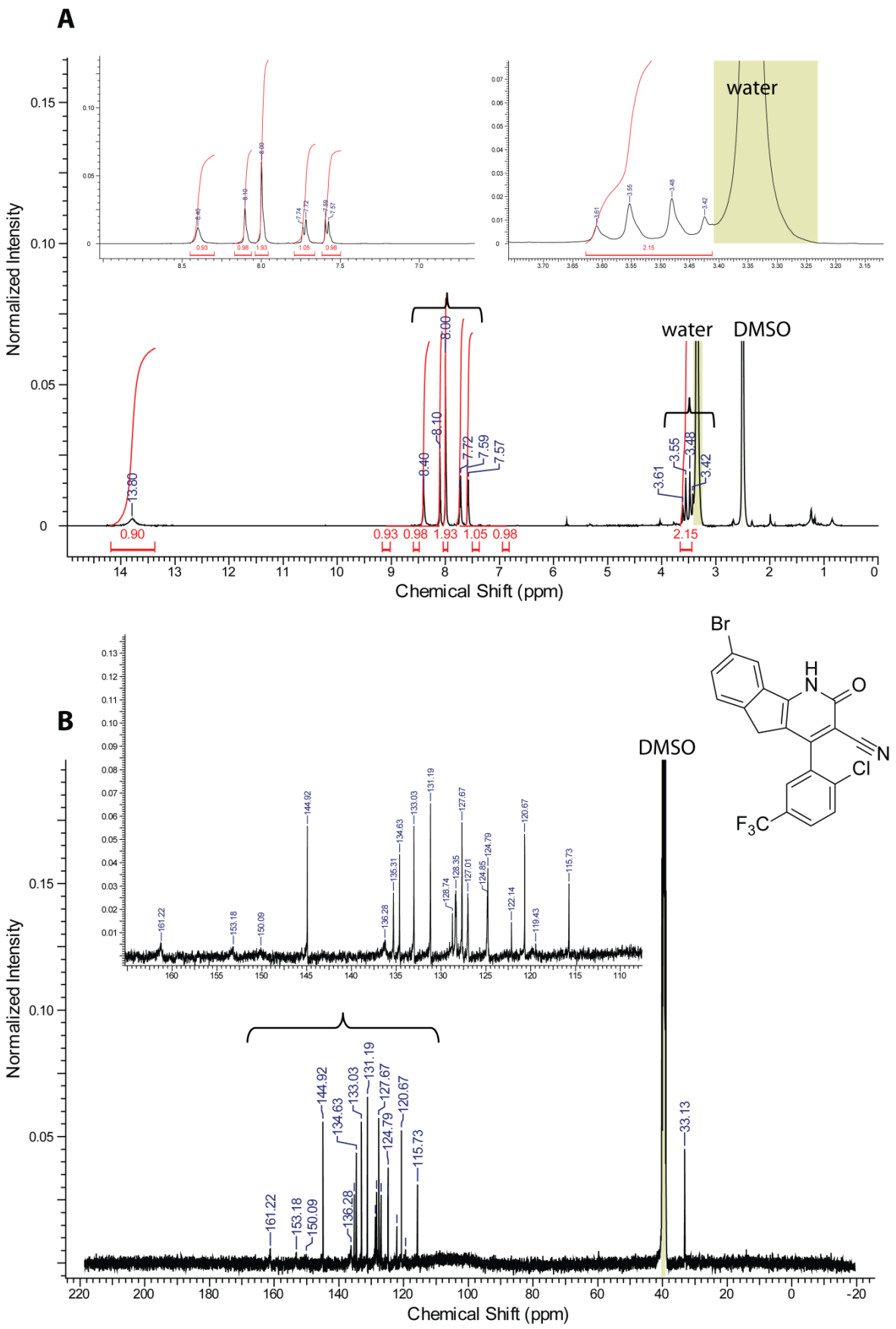
A
Normalized Intensity
Chemical Shift (ppm)
water
DMSO
13.80
8.40
8.10
8.00
7.72
7.59
7.57
3.61
3.55
3.48
3.42
0.90
0.93 0.98 1.93 1.05 0.98
2.15
B
Br
H
N
O
N
Cl
F3C
DMSO
161.22
153.18
150.09
144.92
136.28
135.31
134.63
133.03
131.19
128.74
128.35
127.67
127.01
124.85
124.79
122.14
120.67
119.43
115.73
33.13

C

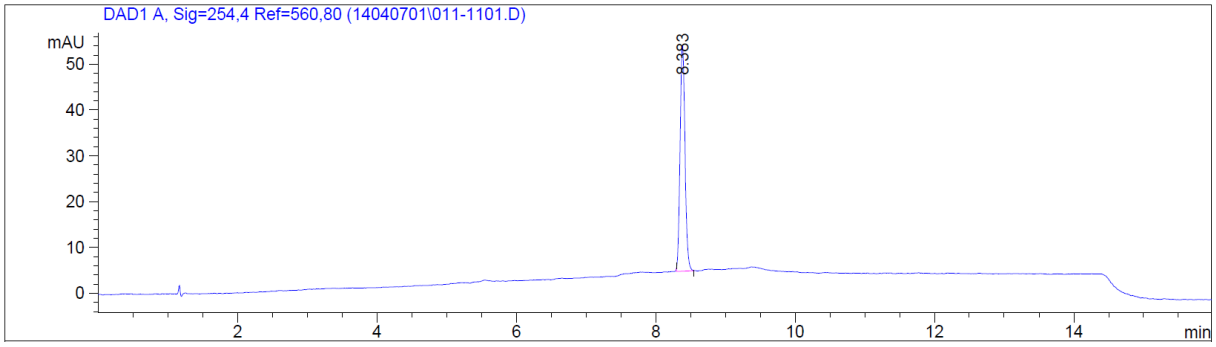

Figure S4. ^{1}H NMR,^{13}C NMR spectra and analytical HPLC chart for **11** are in (A), (B) and (C) respectively. The red values and lines show the integration to number of protons.

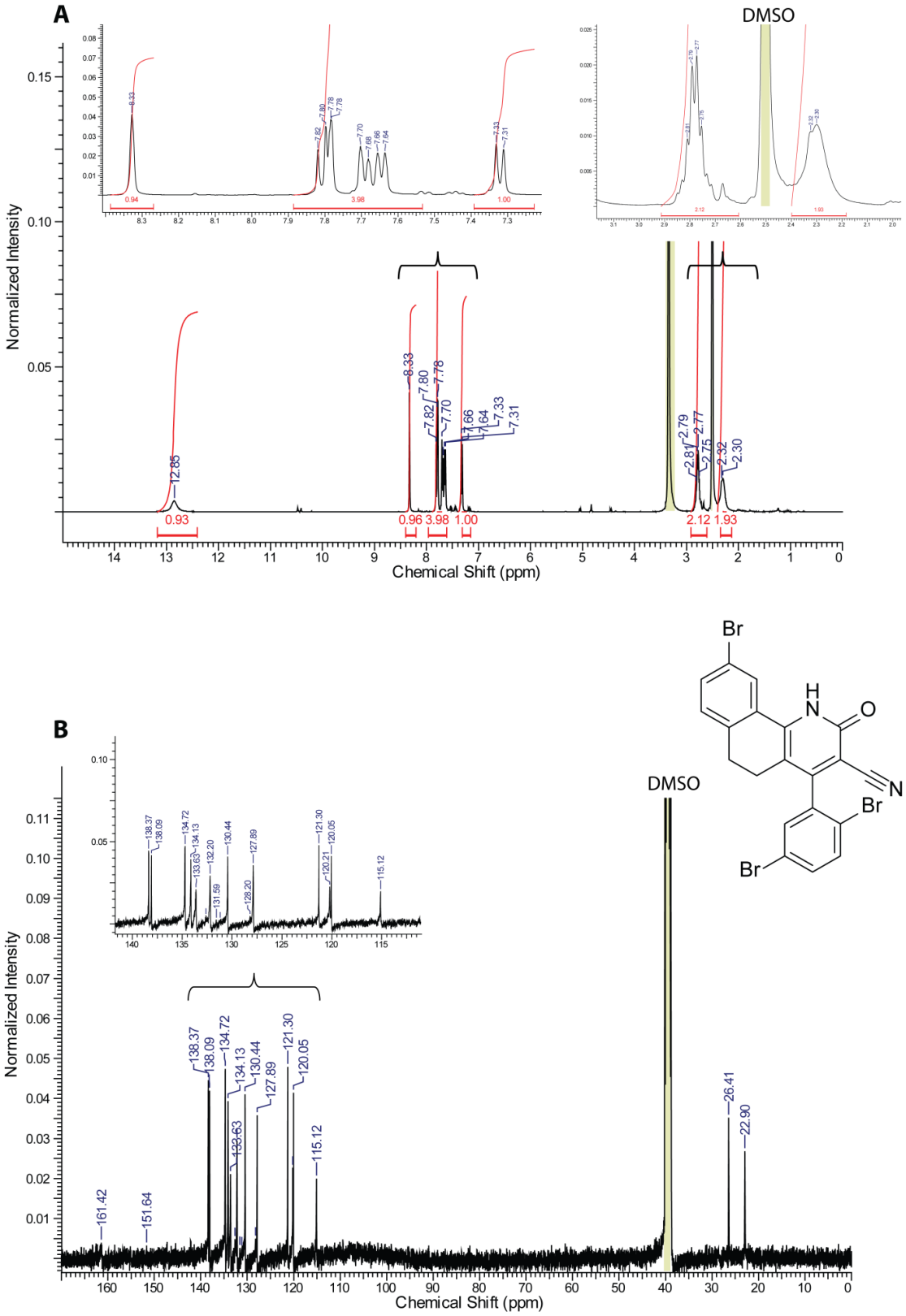

Figure S5. ^{1}H NMR and ^{13}C NMR spectra for **15** are in (A) and (B), respectively. The red values and lines show the integration to number of protons.

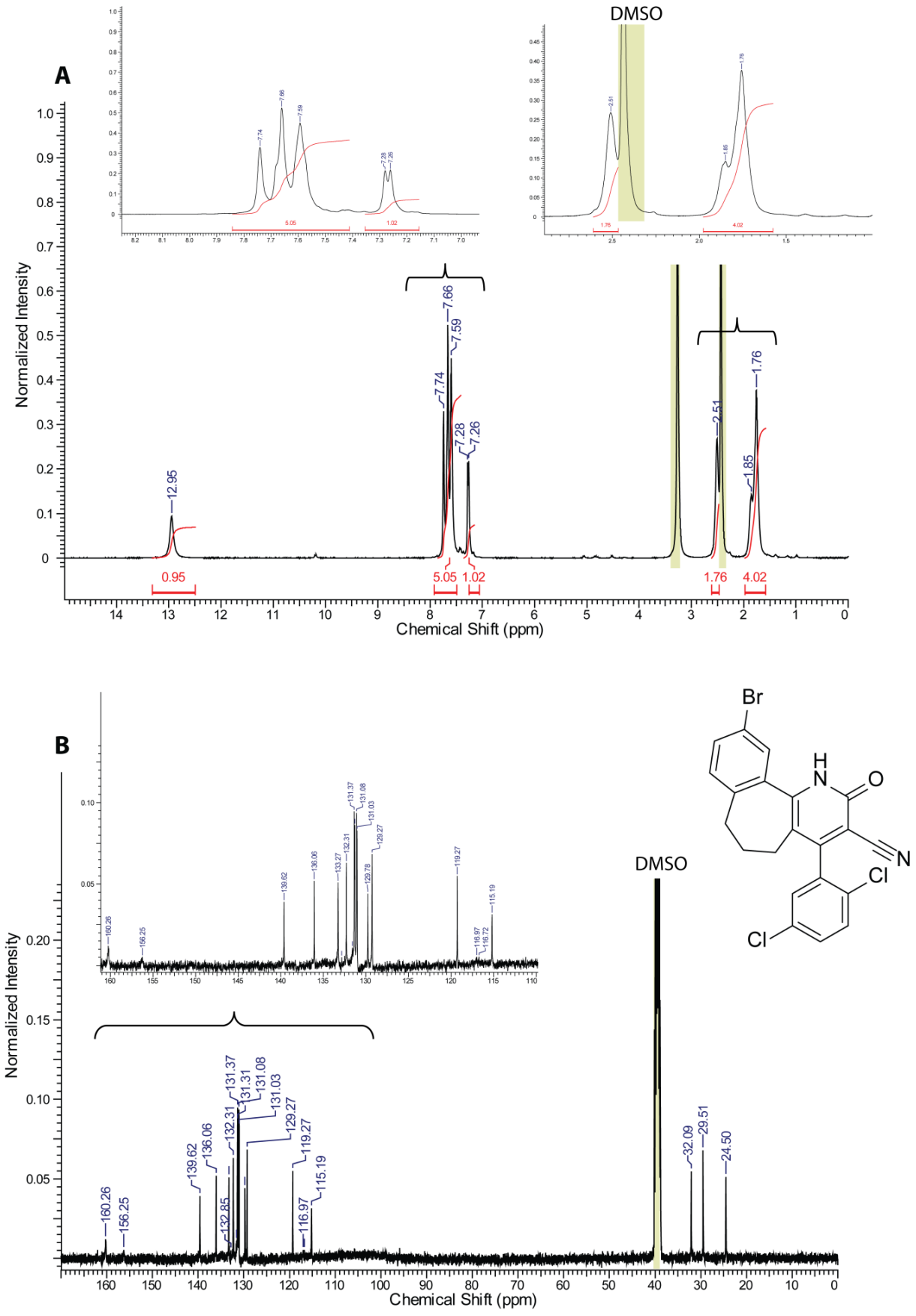
A
DMSO
Normalized Intensity
Chemical Shift (ppm)
12.95
7.74
7.66
7.59
7.28
7.26
2.51
1.85
1.76
0.95
5.05
1.02
1.76
4.02
B
DMSO
Br
H
N
O
N
Cl
Cl
160.26
156.25
139.62
136.06
132.85
132.31
131.37
131.31
131.08
131.03
129.27
119.27
116.97
115.19
32.09
29.51
24.50

C

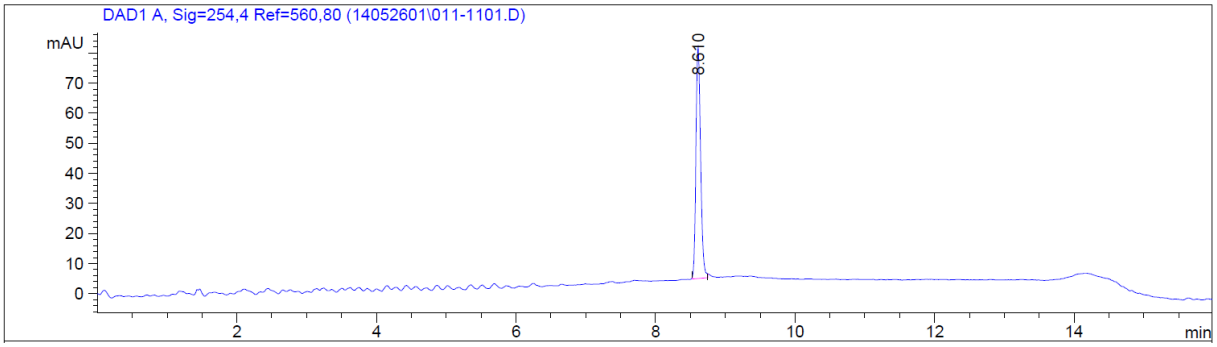

Figure S6. ^{1}H NMR,^{13}C NMR spectra and analytical HPLC chart for **19** are in (A), (B) and (C) respectively. The red values and lines show the integration to number of protons.

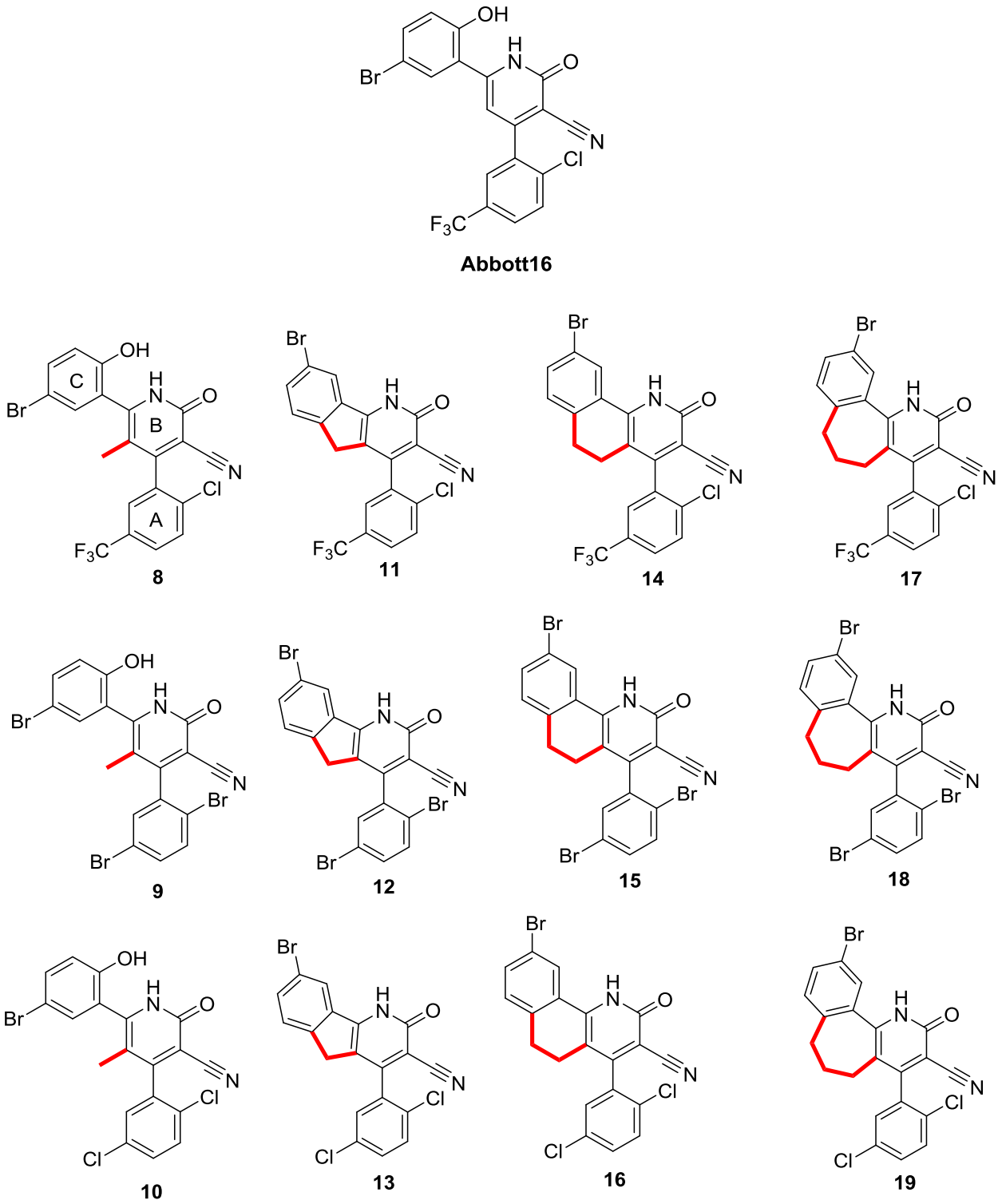

Figure S7. Chemical structures of the synthesized compounds used in the fluorescence assay.

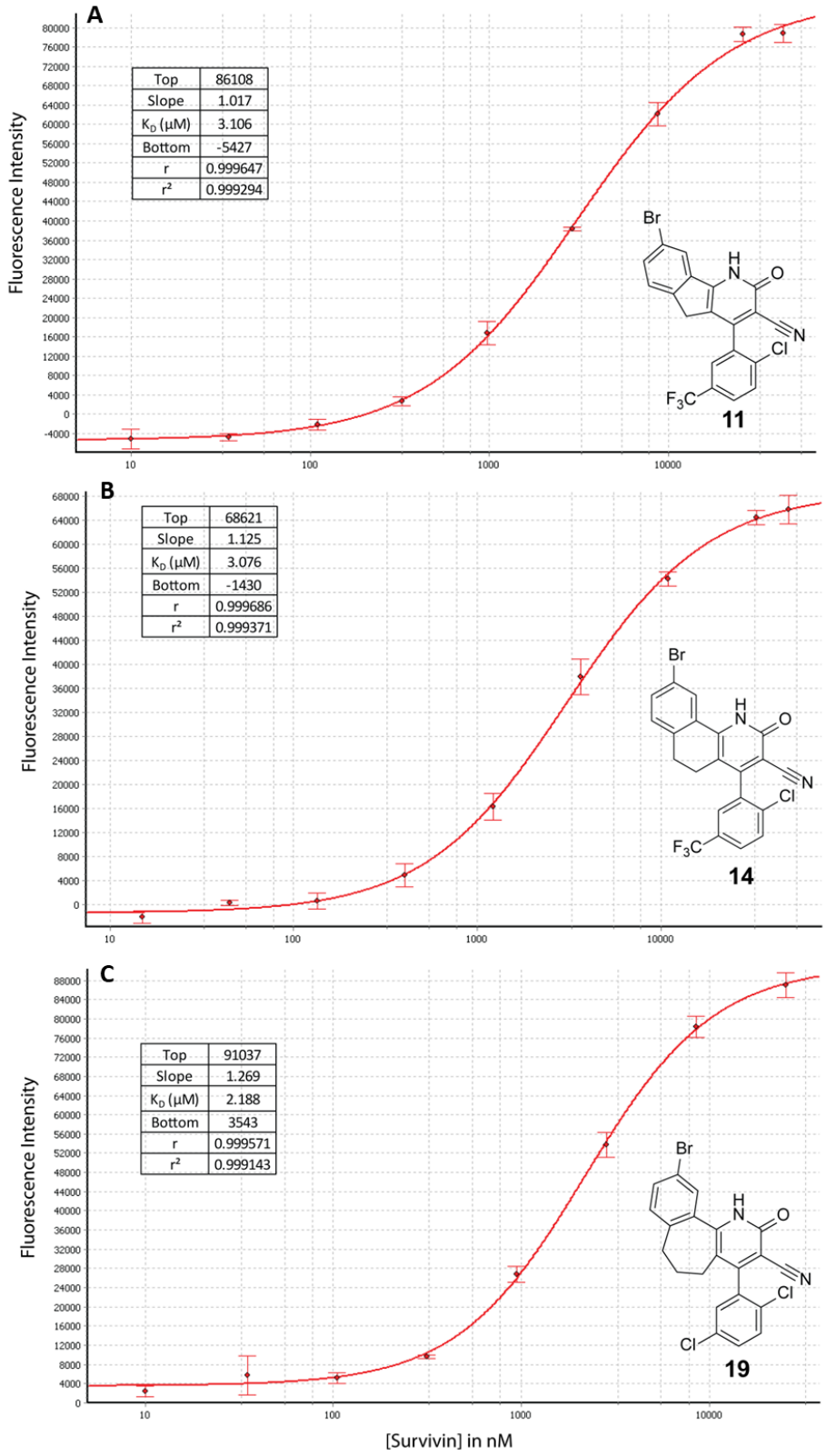

Figure S8. Curves for the fluorescence assay based on four parameter fit model (sigmoidal model) for compounds **11**, **14** and **19** for A, B and C, respectively. The error bars are presented as the standard deviation (SD). All the measurements were at least conducted in triplicates.

The fluorescence data in **Figure S8** were fitted to a four-parameter sigmoidal curve model as shown by the following equation and representative curve [2]:

$$Y = Bottom + \frac{(Top - Bottom)}{1 + \left(\frac{K_D}{x}\right)^{slope}}$$

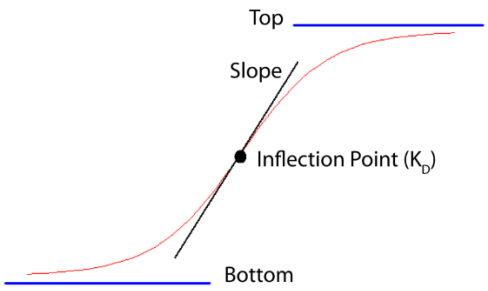

Where "Bottom" is the minimum of the curve, "Top" is the maximum of the curve, and "K_D" is the dissociation constant which is derived from the inflection point.

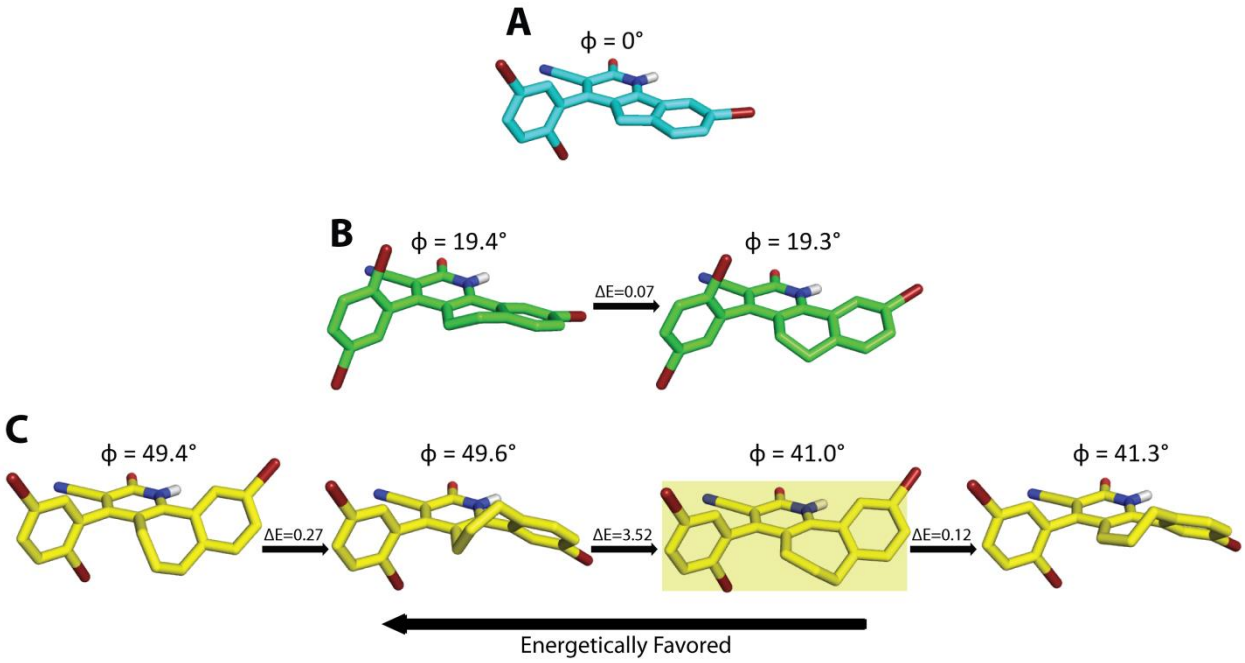

Figure S9. Main ring conformations (low energy) of the five, six, seven-membered rigidized systems represented by A, B and C respectively in vacuum. The tri-bromo derivatives (i.e. **12**, **15**, **18**) were used in this **Figure** with similar pyridone ring perspective. ϕ is the dihedral angle between rings B & C. The highlighted ring conformer for **18** is selected for the best docking pose for all **17-19** compounds. ΔE (kcal/mol) is the difference in potential energy between two conformations. Other compounds show comparable – to a certain extent – ring conformations and energetics. Non-polar hydrogens are omitted for clarity.

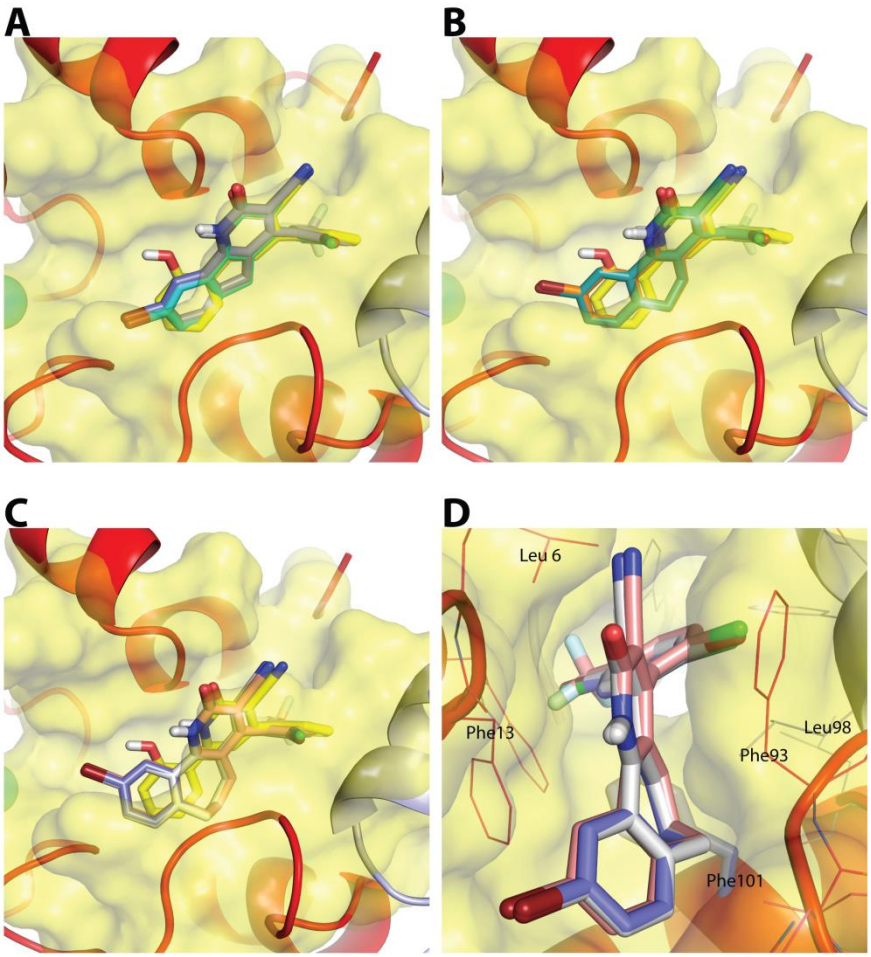

Figure S10. (A), (B) and (C) show overlay of the best docking poses of the five, six and seven-membered rigidized compounds, respectively, with **Abbott8** (yellow sticks) in the binding site of the MD representative structure. Such poses show one similar ring conformation per rigidized system. (D) Best poses of the seven-membered rigidized compounds **17-19** show certain ring conformation in the narrow cleft of the binding site (formed by Phe93 and Phe13). Non-polar hydrogens (for compounds) and all hydrogens (for residues) are omitted for clarity.

References

1. Shao JY, Tanner SW, Thompson N, Cheatham TE. Clustering molecular dynamics trajectories: 1. Characterizing the performance of different clustering algorithms. *Journal of Chemical Theory and Computation.* 2007;3(6):2312-2334.
2. CLARIOstar (BMG labtech). *http://wwwbmglabtechcom/ "user manual".*